0026-895X/01/6006-1356–1364$3.00
MOLECULAR PHARMACOLOGY
Copyright © 2001 The American Society for Pharmacology and Experimental Therapeutics
*Mol Pharmacol* 60:1356–1364, 2001

Vol. 60, No. 6
731/946983
*Printed in U.S.A.*



# Ryanodine Receptor Dysfunction in Hearts of Streptozotocin-Induced Diabetic Rats

KESHORE R. BIDASEE, Ü. DENIZ DINÇER, and HENRY R. BESCH, JR.

*Department of Pharmacology and Toxicology, Indiana University School of Medicine, Indianapolis, Indiana (K.R.B., H.R.B.); and Department of Pharmacology, Faculty of Pharmacy, University of Ankara, Tandogan, Ankara, Turkey (Ü.D.D.)*

Received December 1, 2000; accepted August 30, 2001

This paper is available online at http://molpharm.aspetjournals.org

## ABSTRACT

Studies have shown that evoked calcium release from sarcoplasmic reticulum is compromised in diabetic rat hearts. The present study was undertaken to determine whether this decrease might be ascribed to a reduction in expression and/or alteration in function of ryanodine receptor (RyR2) and whether changes could be minimized with insulin treatment. Hearts were isolated from 4- and 6-week streptozotocin (STZ)-induced diabetic, 4-week diabetic/2-week insulin-treated, and age-matched control rats. RyR2 mRNA and protein levels were determined using reverse transcription-polymerase chain reactions and polyacrylamide gel electrophoresis, respectively, whereas the functional integrity of RyR2 was assessed from their ability to bind [$^3$H]ryanodine. RyR2 protein was unchanged with up to 6 weeks of untreated STZ-induced diabetes. Two weeks of insulin treatment initiated after 4 weeks of diabetes increased RyR2 mRNA levels by 42% and RyR2 protein levels by 45 to 61%. At equivalent amounts, RyR2 protein from 4-week STZ-induced diabetic rat hearts bound 9% less [$^3$H]ryanodine than age-matched control rats (74.1 $\pm$ 3.9 versus 67.4 $\pm$ 3.4 fmol/$\mu$g RyR2), whereas that from 6-week STZ-diabetic rats bound 36% less than control rats (47.9 $\pm$ 4.8 versus 74.2 $\pm$ 4.5 fmol/$\mu$g RyR2, $p < 0.05$). RyR2 from insulin-treated animals bound significantly less [$^3$H]ryanodine than control rats (65.2 $\pm$ 4.9 fmol/$\mu$g RyR2, $p < 0.05$). Apparent affinity of ryanodine for RyR2 was similar among all groups ($K_d \approx 1.04 \pm 0.08$ nM). Because expression did not change significantly but ryanodine binding decreased, these data suggest that the functional integrity of RyR2 is compromised in diabetic rat hearts, and these changes can be attenuated with 2 weeks of insulin treatment.

Despite compliance with mainstay insulin and/or oral hypoglycemic therapies, the incidence of congestive heart failure is 2- to 5-fold higher in the diabetic population than it is in subjects without diabetes, and the increased risk is independent of coronary artherosclerosis and/or hypertension (Rubler et al., 1972; Bell, 1995). This specific diabetic cardiomyopathy (DC) is seen in later stages as a reduction in heart rate, a decrease in rate of left ventricular systolic pressure development and diminished peak tension, an elevation in end-diastolic pressure (from slower relaxation kinetics), and a concomitant decrease in cardiac output (Mahgoub and Abd-Elfattah, 1998).

Cardiac contraction depends critically on the integrity of the sarcoplasmic reticulum (SR). After depolarization, rapid release of calcium ions from the SR via type 2 ryanodine receptor calcium-release channels (RyR2) is a prerequisite for efficient contraction. Similarly, re-uptake of the released calcium into the SR via $Ca^{2+}$/$Mg^{2+}$-ATPase pumps (SERCA 2a) is crucial for cardiac relaxation (Bers, 1991; Berridge, 1997). Proteins involved in storage of calcium inside the lumen of the SR may also be important (for review, see Kiriazis and Kranias, 2000). As such, it is conceivable that a decrease in expression and/or activity of one or more of SR proteins may contribute to diminish peak tension and slower relaxation kinetics seen in DC (de la Bastie et al., 1990; Davidoff and Ren, 1997; Klautz et al., 1997).

SERCA2a is the most studied of SR proteins and its is generally accepted that its activity decreases with diabetes (Ganguly et al., 1983, Lopaschuk et al., 1983). However, it is still not clear whether this decrease results from a decrease in expression (Russ et al., 1991; Zarain-Herzberg et al., 1994), diabetes-induced changes to its secondary/tertiary structures, a decreased steady-state phosphorylation of phospholamban (resulting perhaps from alteration in the complement of $\beta$-adrenoceptors; Dinçer et al., 2001), increase in the ratio of phospholambam to SERCA2a (Kiriazis and Kranias, 2000; Teshima et al., 2000), or combinations thereof.

Yu and McNeill (1991) suggested that RyR2 may be implicated in the genesis and progression of DC when they found

This work was supported in part by Grant R01-HL66898 from the National Institutes of Health, the Biomedical Research Committee, Indiana University School of Medicine, and the Ralph W. and Grace M. Showalter Trust.

**ABBREVIATIONS:** DC, diabetic cardiomyopathy; MV, membrane vesicles; RyR2, type 2 ryanodine receptor; PCR, polymerase chain reaction; STZ, streptozotocin; SR, sarcoplasmic reticulum; AGEs, advanced glycation end products; bp, base pair(s); NPH, neutral protamine hagedorn; Tfl, *Thermus flavus*.

that potentiation after rest (or Woodworth staircase: an enhanced contraction that follows a long pause between contractions) was significantly reduced in hearts (papillary muscles) from 6-week STZ-induced diabetic rats. In follow-up studies, these workers (Yu et al., 1994) found that SR membranes from STZ-diabetic rat hearts bound less [$^3$H]ryanodine (expressed as a decrease in $B_{max}$) than those from age-matched control rats and suggested that this may result from a decrease in the density of RyR2 protein on SR membranes. In a recent study, Teshima et al. (2000) found that 3 weeks of untreated diabetes did not alter mRNA levels encoding RyR2 compared with age-matched control rats. Although suggestive, mRNA levels do not always parallel steady-state protein levels.

The principal goal of the present study was to determine whether the decrease in [$^3$H]ryanodine binding seen with SR membranes from STZ-induced diabetic rat hearts stems from a reduction in expression and/or a dysfunction of RyR2 protein. We also investigated whether diabetes-induced changes to RyR2 could be minimized with insulin treatment initiated after 4 weeks of untreated diabetes.

## Materials and Methods

**Chemicals and Drugs.** Ryanodine used in this study was isolated from chipped Ryania wood supplied by Integrated Biotechnology Corporation (Carmel, IN) and purified by chromatography to ≥ 98%. [$^3$H]Ryanodine (specific activity 87 Ci/mmol) was purchased from PerkinElmer Life Science Products (Boston, MA). Methohexital sodium (Brevital) and intermediate-acting insulin (NPH Ilentin II) were obtained from Eli Lilly & Co. (Indianapolis, IN). Streptozotocin (STZ) was obtained from Sigma-Aldrich (St Louis, MO). Mouse anti-RyR2 antibodies (MA3–916) were obtained from Affinity Bioreagents Inc. (Golden, CO). All other reagents and solvents used were of analytical grade.

**Induction and Verification of Experimental STZ-Induced Diabetes.** All animal procedures were done in accordance with institutional guidelines established by the Institutional Animal Care and Use Committee, Indiana University School of Medicine. Male Sprague-Dawley rats weighing between 200 and 250 g were purchased from Harlan Laboratories (Indianapolis, IN). After anesthesia (Brevital, 25 mg/kg i.p.), animals were injected via tail veins with a single dose of STZ in 0.1 M citrate buffer, pH 4.5 (45 mg/kg), or citrate buffer only. Three days later, blood glucose levels were determined using a Glucometer II and Glucostix (Peridochrom Glucose GOD-PAP Assay Kit; Roche Molecular Biochemicals, Indianapolis, IN) to ensure induction of diabetes. Throughout this study, all animals were housed individually at 22°C with fixed 12-h light/12-h dark cycles and given free access to food and water.

**Insulin-Treatment Protocols.** Four weeks after the initial STZ injections, diabetic animals were divided randomly into three groups. One group of animals was placed on an insulin regimen (NPH Ilentin II) for 2 weeks. Insulin doses were individually adjusted so as to maintain euglycemic states and varied between 8 and 15 U/kg (sc), given once per day between 9 and 10 AM. Another group of animals continued as nontreated diabetics for 2 additional weeks. The third group of diabetic animals was sacrificed along with age-matched control rats (4 weeks).

**Sample Collection.** All animals were sacrificed by injection of Brevital (75 mg/kg, i.p.). Abdominal cavities were opened and blood samples were collected via the left renal arteries for analysis of plasma glucose, insulin, and hemoglobin $A_{1c}$ content. Animals within each group were further divided into two subgroups of three and ≥six animals, respectively. Crude membrane vesicles were prepared using hearts from each of the larger subgroups. For 4-week age-matched control and 4-week STZ-induced diabetic rats, three preparations were made (two hearts per preparation), and for 6-week age-matched control, 6-week STZ-induced diabetic, and 4-week STZ-diabetic/2-week insulin treated four preparations were made (six hearts per preparation). Total RNA was isolated from individual hearts from the smaller subgroup and reverse transcribed into first strand cDNA (three preparations for each group).

**Isolation and Quantitation of Total RNA.** After sacrifice, hearts designated for isolation of total RNA were removed, quick-frozen by sinking into and covering with powdered dry ice, and then stored at −80°C. Total RNA was later extracted using the procedure provided by Amersham Pharmacia Biotech (Piscataway, NJ) with the Quick Prep total RNA extraction kit. At the end of the isolation procedure, RNA samples were suspended in 1 ml of diethylpyrocarbonate-treated water, pH 7.5, and absorbance values were determined spectrophotometrically at 260 nm ($\lambda_{260}$). The amount of total RNA in each sample was then determined using the formula, [RNA] = $A_{\lambda 260}$ × dilution factor × 40 μg/ml. Absorbance values of RNA samples were also determined at $\lambda_{280}$ and only RNA samples with $A_{\lambda 260}/A_{\lambda 280}$ ratios greater than 1.8 were used for synthesis of first strand cDNA. RNA samples were also electrophoresed using denaturing formamide/formaldehyde agarose gels to ensure that minimum degradation occurred during the isolation and relative ethidium bromide intensities of 28S and 18S ribosomal RNA bands parallel absorbance values.

**Preparation of First Strand cDNA via Reverse Transcriptase Reactions.** RNA of acceptable quality ($A_{\lambda 260}/A_{\lambda 280}$ values greater than 1.8 and possessing distinct 28S and 18S ribosomal RNA on formamide/formaldehyde gels) were used as templates for the synthesis of first strand cDNA. Briefly, 1 μl of oligo $dT_{15}$ was added to an equivalent amount of total RNA isolated from control, diabetic, and insulin-treated rat hearts. The mixtures were then heated for 10 min at 70°C in a thermocycler (model 2400; PerkinElmer, Norwalk, CT). At the end of this time, the samples were transferred to an ice bath to permit selective binding of the oligo $dT_{15}$ to the poly-A tail of the mRNA. Thereafter, 10 μmol of deoxynucleotide triphosphate (dNTP), 200 μmol of dithiothreitol, 4 μl of 5× first strand buffer, 1 μl of Superscript II, and 1 μl of RNasin were added, followed by water to a final volume of 20 μl. The tubes were then heated for 45 min at 42°C for reverse transcription followed by 5 min at 94°C for denaturation. First strand cDNA samples were cooled and stored at −80°C until use.

**Amplification of cDNA Encoding RyR2.** Gene-specific primers were used in PCR to determine the amount of RyR2 transcript in each sample. For this, 5 μl of 10× Tfl buffer, 55 μmol of $MgSO_4$, 100 μmol of dNTP, 0.2 μl of Tfl DNA polymerase (5 U/μl; Promega, Madison, WI), 1 μl of respective cDNA (control, diabetic, or insulin-treated), and 25 pmol of sense and anti-sense RyR2 and β-actin primers were added to PCR tubes. Diethylpyrocarbonate-treated water was added to each tube for a final volume of 50 μl. PCRs were then carried out using the program: 5 min of denaturation (94°C), 1 min of annealing (54°C), and 2 min of extension (72°C), repeated for a total of 37 cycles. At the end of the reaction, 5 μl from each PCR reaction was mixed with Blue/Orange loading dye (Promega) and electrophoresed for 1.5 h at 100 V using 2% agarose gels containing ethidium bromide. The gels were visualized and photographed (Gel-Doc 1000 complete with Molecular Analyst software; Bio-Rad, Hercules, CA). Images were opened using Scion Imaging software (version 1.62; Frederick, MD), and the band intensities were quantitated and used as measures of RyR2 mRNA concentrations.

Sense ($_{5160}$GTGTTTGGATCCTCTGCAGTTCAT$_{5183}$) and anti-sense ($_{5762}$AGAGGCACAAAGAGGAATTCGG$_{5741}$) primers for RyR2 were designed based on rabbit RyR2 cDNA sequences (GenBank accession number M59743). Primers used for amplifying a segment of β-actin cDNA were designed from nucleotide sequence encoding rat cytosolic β-actin gene (accession number V01217) and are as follows: sense ($_{2750}$CGTAAAGACCTCTATGCCA$_{2768}$) and anti-sense ($_{3222}$AGCCAT GCCAAATGTCTCAT$_{3203}$).

**Characterization of the Rat RyR2 PCR Product.** The identity of PCR product encoding a segment of RyR2 was established by comparing its nucleotide sequences with those in GenBank. Twenty-four PCRs were carried out as described above except that only primers for RyR2 were used. At the end of the reaction, the contents of the tubes were pooled, diluted 1:1 with dye, and electrophoresed using 2% agarose gel (low melting). The gels were irradiated ($\lambda_{366}$) and the bands of interest were excised. The DNA was then extracted from the agarose using a QIAEX II gel extraction kit (QIAGEN Inc., Valencia, CA) according to the manufacturer's protocol. DNA was ethanol precipitated to remove residual salts and its nucleotide sequence was determined using an ABI 377 DNA sequencer (Applied Biosystems, Foster City, CA). Experimentally obtained sequences were then compared with published sequences using the Web-based alignment program MultAlin (http://www.toulouse.inra.fr/multalin.html). Endonuclease restriction mapping was also conducted as another way of confirming the identity of the PCR product.

**Preparation of Membrane Vesicles.** Membrane vesicles (MV; mixture of sarcolemma and sarcoplasmic reticular membranes) were prepared from rat hearts using procedures described previously (Bidasee et al., 2000), with the exception that the tissue was homogenized six times for 10 s instead of three times for 30 s at Polytron setting 6.5.

**RyR2 Binding of [$^3$H]Ryanodine.** The functional integrity of RyR2 on MV prepared from rat hearts was determined from their ability to bind [$^3$H]ryanodine. Briefly, 0.1 mg/ml SR membrane protein from 4- and 6-week control rats, 4- and 6-week STZ-diabetic, and 4-week STZ-induced diabetic/2-week insulin treated animals were incubated in binding buffer (500 mM KCl, 20 mM Tris-HCl, and 200 $\mu$M $CaCl_2$, pH 7.4) for 2 h at 37°C with 6.7 nM [$^3$H]ryanodine and increasing amounts of unlabeled ryanodine up to 300 nM. After incubation, vesicles were filtered and washed, and the amount of [$^3$H]ryanodine bound to RyR2 was determined using liquid scintillation counting. Nonspecific binding was determined simultaneously by incubating vesicles with 1000 nM unlabeled ryanodine. $IC_{50}$ values were determined using the binding analysis program Prism 2.0 (GraphPad Software Inc., San Diego, CA), whereas $K_d$ values were ascertained using the Cheng-Prussoff relationship (Cheng and Prusoff, 1973): $K_d = IC_{50} / (1 + [L] / K_L)$, where L is the concentration of [$^3$H]ryanodine used (6.7 nM) and $K_L$ is the equilibrium dissociation constant of [$^3$H]ryanodine (1.2 nM for RyR2; see Bidasee et al., 2000).

**Determination of RyR2 Content in MV Preparations.** Two steps were used to determine the amount of RyR2 protein in each MV preparation. In the first step, 100 $\mu$g of protein from each MV preparation was solubilized with gel-dissociation medium (62.5 mM Tris base, 6% SDS, 20% glycerol, and 0.002% bromphenol blue), boiled for 10 min and electrophoresed on 4 to 20% linear gradient polyacrylamide gels (Bio-Rad) for 3.5 h at 150 V. At the end of this time, the gels were stained with 0.25% Coomassie blue dye for 1 h, destained for 16 h, and then dried between blotting paper and cellophane. Images of gels were captured and stored using the computer program Photoshop 5.0 (Adobe Systems, Mountain View, CA). Stored gels were then open using the analysis program Scion Image 1.62c (based on NIH Image, Bethesda, MD). The intensities of Coomassie-stained RyR2 bands were determined using the rectangular box method (a closed loop was also hand drawn around bands that were too irregular for the rectangular box method). The average intensity of identical size rectangular boxes (or close loops) above and below each RyR2 band on the gel was used as its corresponding background staining and subtracted.

In the second step, intensities of Coomassie-stained RyR2 in MV preparations were interpolated on RyR2 calibration curves to determine their concentration equivalent. For this, purified RyR2 (0.5–3 $\mu$g) was added to gel-dissociation medium and electrophoresed on 4 to 20% linear gradient polyacrylamide gels as described above. At the end of this time, the gels were Coomassie-stained, destained, and then dried. Images of calibration gels were captured using Adobe Photoshop 5.0 and the intensities of RyR2 bands were determined using Scion Image 1.62c. Background staining was determined as described above and subtracted. Several calibration curves were run on polyacrylamide gels for quantitation of RyR2 in 4-week control/4-week STZ diabetic and 6-week control/6-week STZ diabetic/4-week STZ diabetic/2-week insulin-treated samples.

**Confirmation of Relative Levels of RyR2 in MV Preparations.** Western blot analyses were also used to confirm relative levels of RyR2 in each MV preparation. Briefly, 100 $\mu$g of MV from each of the five samples were dissolved in gel dissociation medium and electrophoresed as described above. The proteins were then transferred overnight (100 mA) onto polyvinylidene difluoride membranes (Immobilon; Millipore Corporation, Bedford, MA) using a semidry electroblotter (Panther; Owl Scientific Inc., Woburn, MA) with buffer consisting of 10 mM cyclohexylamino-1-propanesulfonic acid/0.01% SDS in 10% methanol, pH 9.0. The next day, the membranes were blocked (0.01 M Tris-HCl, 0.05 M NaCl, 5% nonfat dry milk, and 0.04% Tween 20, pH 7.4, for 1 h), washed with phosphate-buffered saline, pH 7.4, and incubated for 20 h with mouse anti-RyR2 antibodies at 4°C. At the end of this time the membranes were again washed and incubated for 2 h at room temperature with anti-mouse IgG-horseradish peroxidase (Roche Molecular Biochemicals, Indianapolis, IN). Membranes were then incubated for 1 min with enhanced chemiluminescence (ECL; Amersham Pharmacia Biotech, Piscataway, NJ) and exposed to X-ray films (Hyperfilm; Amersham Pharmacia Biotech). Auto-radiograms were developed after 10 min. Intensities of RyR2 signals on films were then measured and used as relative levels of RyR2 in 100 $\mu$g of each MV preparation.

**Data Analysis and Statistics.** Differences among values from each of control, STZ-induced, and insulin-treated diabetic rats were evaluated by one-way analysis of variance followed by Neuman-Keul's test. The data shown are means ± S.E.M. Results were considered significantly different if $p < 0.05$.

## Results

**Induction of Experimental STZ-Induced Diabetes Mellitus.** Some characteristics of the animals used in this study are summarized in Table 1. All rats injected with STZ had blood glucose levels greater than 25 mM within 3 days. At the end of the in vivo experimental protocol, analysis of

TABLE 1
General characteristics of control, streptozotocin-induced and insulin-treated diabetic rats
Values shown are mean ± S.E.M.

| Parameter | Age-Matched Control Rats | | 4-Week STZ-Induced Diabetic ($n$ = 9) | 6-Week STZ-Induced Diabetic ($n$ = 27) | 4-Week STZ-Induced Diabetic/2-Week Insulin Treated ($n$ = 27) |
|---|---|---|---|---|---|
| | 4 Weeks ($n$ = 10) | 6 Weeks ($n$ = 28) | | | |
| Body weight (g) | 292.8 ± 6.4 | 333.3 ± 15.9 | 219.5 ± 3.9* | 215 ± 8.3* | 360.2 ± 7.3 |
| Heart weight (g) | 1.0 ± 0.1 | 1.0 ± 0.1 | 0.9 ± 0.1 | 0.8 ± 0.09 | 1.1 ± 0.5 |
| Plasma glucose (mM) | 5.8 ± 0.3 | 5.9 ± 0.2 | 34.1 ± 1.0* | 35.1 ± 1.0* | 5.7 ± 0.4 |
| Insulin (ng/ml) | 2.6 ± 0.2 | 2.7 ± 0.2 | 0.07 ± 0.01* | 0.07 ± 0.01* | 2.3 ± 7 |
| Hemoglobin $A_{1c}$ (%) | 5.0 ± 0.3 | 4.8 ± 0.2 | 9.6 ± 0.2* | 9.7 ± 0.2* | 5.9 ± 1.3 |

* Significantly different from control and insulin-treated animals.

plasma from diabetic animals showed increased levels of glucose and hemoglobin $A_{1c}$ and a decrease in insulin level. After 4 weeks of untreated diabetes mean body weights were significantly lower in diabetic rats than control rats. Mean body weights decreased further after 6 weeks of untreated diabetes. Heart weight to body weight ratios were significantly higher in 4-and 6-week diabetic rats compared with control rats (4.10 versus 3.22 mg/g and 4.46 versus 3.00 mg/g, respectively). This ratio returned to near control values with insulin treatment (3.28 versus 3.00 mg/g).

**Quantitation of Total RNA Isolated from Rat Hearts.** Minimum degradation of total RNA occurred during the isolation procedures, as indicated by $A_{\lambda 260}/A_{\lambda 280}$ values ranging between 1.88 to 1.95 and distinct 28S and 18S ribosomal RNA in denaturing formamide/formaldehyde agarose gels (data not shown). However, we did find that the amount of total RNA isolated from 4- and 6-week STZ-induced diabetic rat hearts were significantly less than that isolated from age-matched control rats (486 ± 120 and 256 ± 144 $\mu$g compared with 640 ± 72 and 632 ± 72 $\mu$g, respectively). These data are consistent with those in the literature showing that transcription rate of several proteins are slowed in the diabetic heart (Brownsey et al., 1997). The amounts of total RNA isolated from insulin-treated diabetic rat hearts were similar to those from age-matched control rats (656 ± 80 $\mu$g) and are consistent with the observation that insulin replacement stimulates protein synthesis (Wolfe, 2000).

**Quantitation of RyR2 Transcripts.** PCR was used to determine the amounts of RyR2 transcripts in cDNA from control (4- and 6-week), STZ-induced (4- and 6-week), and insulin-treated diabetic rats (4-week STZ-diabetic/2-week insulin-treatment) hearts. After normalization to concomitant $\beta$-actin expression, levels of mRNA encoding RyR2 in hearts from 4- and 6-week STZ-induced diabetic rats were not significantly different from control rats (96 ± 4% of control and 95 ± 7% of control, respectively, Fig. 1). It should be pointed out that RyR2 from 4-week (control and STZ diabetic) and 6-week (control and STZ-diabetic) rats were assayed at different times, hence the reason for differences in ethidium bromide intensities. Interestingly, 2 weeks of insulin treatment significantly increased RyR2 transcripts to levels that were 42 ± 4% greater than age-matched control rats (Fig. 1, lane 5). Although suggestive, an increase transcription is not conclusive evidence that steady-state levels of RyR2 protein increase, because the latter depends on the balance between rates of synthesis and degradation.

**Characterization of PCR Product.** The nucleotide sequence of the PCR product was determined for two reasons. First, the oligo primers used in the PCR were designed based on rabbit RyR2 cDNA sequence. Secondly, this sequence will provide additional information on the cDNA encoding rat RyR2. After sequencing and alignment, the PCR product exhibited greater than 90% homology with nucleotide sequences encoding rabbit RyR2 (bases 5184 and 5750; Otsu et al., 1990) and human RyR2 (nucleotides 5005 and 5571; Tunwell et al., 1996) (data not shown). Endonuclease restriction mapping also generated predicted size fragments based on experimentally derived sequence. Digestion with *Sma*I generated two fragments of 380 and 222 bp, *Pst*I generated 482- and 120-bp fragments and *Bam*HI generated two fragments of sizes 550 and 52-bp (data not shown). These data confirm that the product generated in PCR resulted from specific amplification of cDNA encoding rat RyR2. The nucleotide sequence of this PCR product is listed in GenBank under accession number AF363960.

**RyR2 Binding of [$^3$H]Ryanodine.** Ryanodine binding assays were used to assess the functional integrity of RyR2 from each of control (4- and 6-week), STZ-induced (4- and 6-week), and insulin-treated diabetic MV preparations. As shown in Fig. 2, MV from 4- and 6-week age-matched control rats bound 79.5 ± 4.16 and 79.9 ± 4.8 fmol of [$^3$H]ryanodine/100 $\mu$g of membrane protein, whereas those from 4- and 6-week STZ-induced diabetic bound significantly less [$^3$H]ryanodine and the extent of the decrease was dependent on the duration of untreated diabetes (66.9 ± 3.4 and 49.8 ± 5.0 fmol of [$^3$H]ryanodine/100 $\mu$g of membrane protein). On the other hand, MV protein from insulin-treated STZ-diabetic animals bound 38% more [$^3$H]ryanodine than those from control rats (109.7 ± 8.3 fmol of [$^3$H]ryanodine/100 $\mu$g of membrane protein).

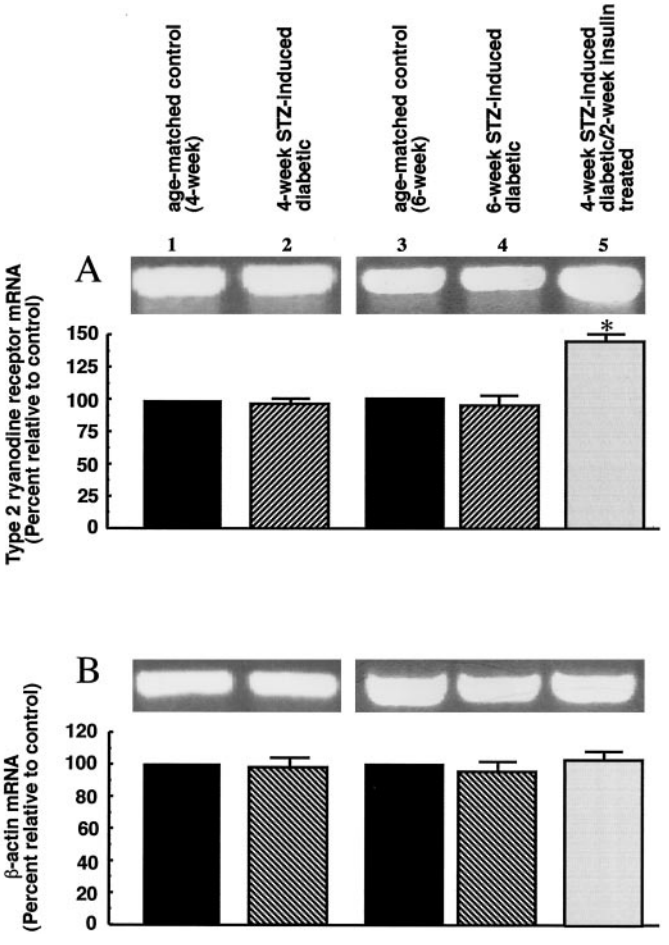


**Fig. 1.** PCR products obtained using cDNA from 4- and 6-week STZ-induced, 4-week STZ-induced/2-week insulin-treated diabetic, and age-matched control rat hearts. Total RNA was reverse-transcribed using oligo $dT_{15}$ and first strand cDNA was subjected to amplification by PCR using RyR2 and $\beta$-actin-specific primers. A, representative sample of PCR product generated using RyR2 primers. Signal intensities are normalized to concomitant $\beta$-actin and are relative to those of age-matched control rats. B, representative sample of PCR product generated using $\beta$-actin primers and relative quantitation of signal intensities. Values shown are means ± S.E.M. obtained from ≥ three experiments performed using at three different cDNA preparations. PCR products were of expected sizes: 602 bp for RyR2 and 387 bp for $\beta$-actin. * denotes value significantly different from control and STZ-induced diabetic rats.

Although the capacity of RyR2 from 4- and 6-week age-matched control rats and insulin-treated animals to bind [$^3$H]ryanodine was significantly greater than those from 4- and 6-week STZ-induced diabetic animals, the apparent affinity of ryanodine for RyR2 from these five experimental groups was essentially identical ($IC_{50}$ = 6.9 ± 0.5 nM; Fig. 3). Using the Cheng Prusoff equation, $K_d$ values were calculated to be 1.04 ± 0.08 nM.

**Quantitation of RyR2 Protein in MV from Rat Hearts.** Denaturing polyacrylamide gel electrophoresis was used to quantitate the amount of RyR2 in 100 μg of each MV preparation. Shown in Fig. 4A are the Coomassie-stained protein bands present in 100 μg of MV from 4-week age-matched control and 4-week STZ-diabetic animals (left panel) and from 6-week control, 6-week STZ-diabetic, and 4-week STZ-diabetic/2-week insulin-treated animals (right panel). Under conditions used in this study, RyR2 exhibits the slowest electrophoretic mobility and represents only a small fraction of the total proteins present in MV preparations. It should also be pointed out that MV from 4-week control and 4-week STZ-diabetic animals were electrophoresed on polyacrylamide gels at different times from those for 6-week control, 6-week STZ-diabetic, and 4-week STZ-diabetic/2-week insulin-treated animals. Hence the reason for differences in resolution of proteins and degree of Coomassie destaining.

The amount of RyR2 present in 100 μg of each MV preparation was then determined by interpolating Coomassie-stained intensities on RyR2 calibration curves. As an example, Fig. 5 shows that the Coomassie-stained intensity was linearly related to concentration of purified RyR2 protein, over a range of 0.5 to 3 μg RyR2 protein ($r^2$ = 0.991). Several RyR2 calibration curves were generated so as to match as closely as possible, the degree of Coomassie destaining (background staining) for each polyacrylamide gel. The concentration range of RyR2 was chosen so as to encompass the spread of Coomassie-stained intensities observed for RyR2 in all MV preparations.

No significant differences were found in the amount of RyR2 protein present in MV preparations from 4- and 6-week age-matched control and 4- and 6-week STZ-diabetic animals (1073 ± 32 ng, 1077 ± 30 ng, 992 ± 28 ng, and 1041 ± 40 ng per 100 μg of membrane protein, respectively). On the other hand, MV preparations from 4-week STZ-induced diabetic/2-week insulin-treated animals contained 1683 ± 23 ng of RyR2/100 μg of MV protein, an amount that was 56.6% greater than that from age-matched control rats and 65.5% greater than that from STZ-induced diabetic animals (average of 61%).

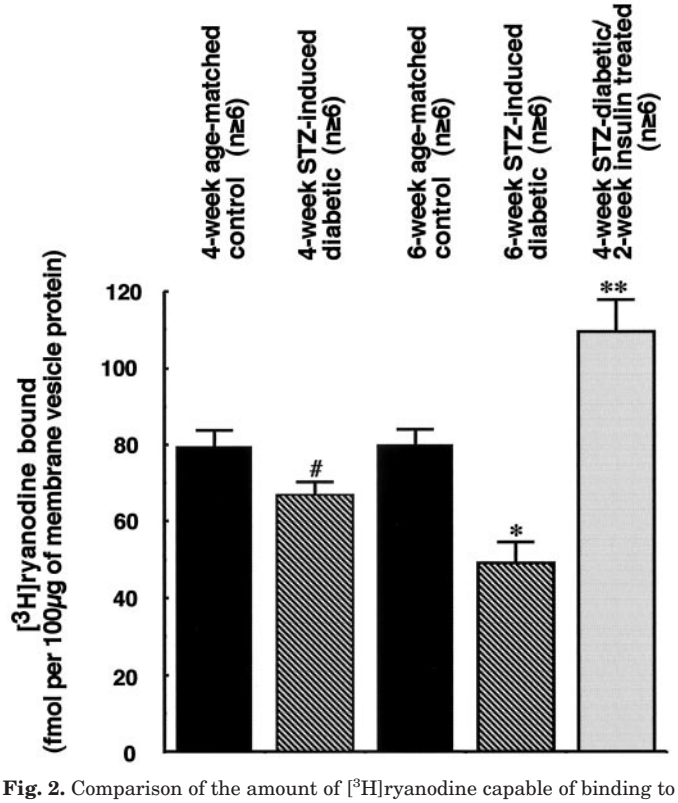


**Fig. 2.** Comparison of the amount of [$^3$H]ryanodine capable of binding to membrane vesicles from 4- and 6-week STZ-induced, 4-week STZ-induced/2-week insulin-treated diabetic, and age-matched control rat hearts. Briefly, MV (0.1 mg/ml) from each of control, STZ-induced diabetic, and insulin-treated diabetic rat hearts were incubated for 2 h at 37°C with 6.7 nM [$^3$H]ryanodine in binding buffer consisting of 500 mM KCl, 0.2 mM $CaCl_2$, and 20 mM Tris-HCl, pH 7.4. After incubation, the vesicles were filtered and washed, and [$^3$H]ryanodine bound to RyR2 was determined by liquid scintillation counting. Data shown are means ± S.E.M. for at least six experiments done in duplicate using three different membrane preparations. # denotes significantly different from control rats (4 and 6 weeks) and insulin-treated. * denotes significantly different from control rats (4 and 6 weeks), 4-week STZ-diabetic, and insulin-treated. ** denotes significantly different from STZ-diabetic (4 and 6 weeks), and age-matched control rats (4 and 6 weeks).

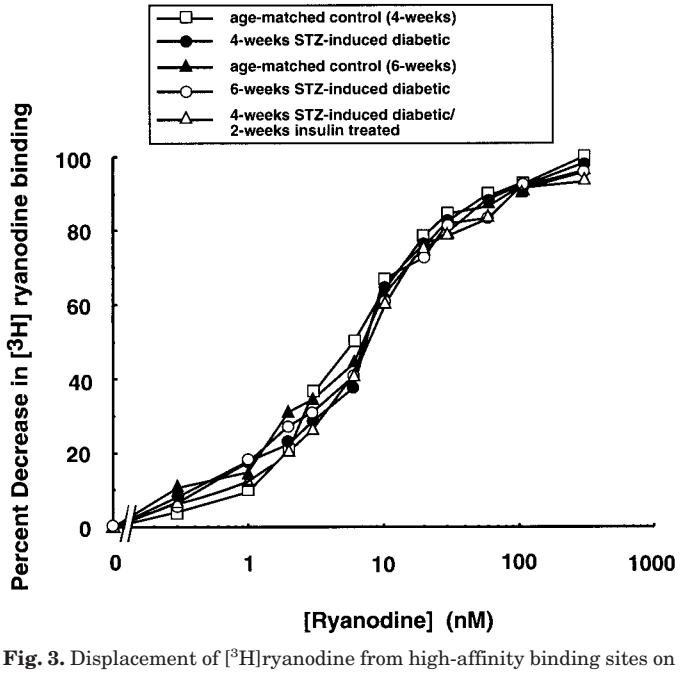


**Fig. 3.** Displacement of [$^3$H]ryanodine from high-affinity binding sites on RyR2. Equilibrium dissociation constant ($K_d$) and $IC_{50}$ values were determined by incubating MV proteins (0.1 mg/ml) from 4- and 6-week control rats, 4- and 6-week STZ-induced, and 4-week STZ-induced diabetic/2-week insulin treated 6-week STZ-induced animals for 2 h at 37°C with 6.7 nM [$^3$H]ryanodine and increasing concentrations of unlabeled ryanodine up to 300 nM. At the end of this time, the vesicles were filtered and washed, and [$^3$H]ryanodine bound was determined by liquid scintillation counting. Nonspecific binding was simultaneously determined by incubating vesicles with 1 μM ryanodine. GraphPad Prism 2.0 was used to calculate $IC_{50}$ values, and these values then used to determine $K_d$ values using the Cheng-Prusoff equation. Data shown are means for at least six experiments done in duplicate using three different membrane preparations. S.E.M. values were less than 5% and were omitted for clarity.

These data parallel those obtained from Western blot analyses using antibodies specific to RyR2 (Fig. 4B). When normalized to the intensity of concomitant age-matched control, STZ-induced diabetes did not significantly alter expression of RyR2 protein. Interestingly, the intensity of RyR2 Western blot from insulin-treated animals were 47.3 ± 7.8% greater than that from control rats.

To more effectively assess the effect of untreated diabetes and insulin treatment on the functional integrity of RyR2 protein, the amount of [$^3$H]ryanodine bound to each MV preparation was normalized to 1 $\mu$g (1000 ng) of RyR2 protein. After this transformation, no significant difference was found in the amount of [$^3$H]ryanodine bound to RyR2 from either 4-week STZ-diabetic and 4-week age-matched control rats (67.4 ± 3.4 versus 74.1 ± 3.9 fmol of [$^3$H]ryanodine/$\mu$g of RyR2 protein; see Fig. 6). On the other hand, RyR2 protein from 6-week STZ-induced diabetic rat hearts bound significantly less [$^3$H]ryanodine than those from corresponding age-matched control rats (47.9 ± 4.8 versus 74.2 ± 4.5 fmol of [$^3$H]ryanodine/$\mu$g of RyR2 protein). It should be mentioned that RyR2 is the only protein in our MV preparations that bind [$^3$H]ryanodine. These data show for the first time is that at equivalent amounts, RyR2 protein from 6-week STZ-induced diabetic animals binds less [$^3$H]ryanodine than those from age-matched control rats. Because [$^3$H]ryanodine is a measure of the functional integrity of RyR2, these data further suggest that the functional integrity of RyR2 is compromised in the hearts of STZ-induced diabetic rats.

Insulin treatment initiated after 4 weeks of untreated diabetes minimizes the loss in [$^3$H]ryanodine binding induced by untreated diabetes (65.2 ± 4.9 fmol of [$^3$H]ryanodine/$\mu$g of RyR2 protein). Compared with RyR2 from 4-week STZ-induced diabetic animals, daily doses of replacement insulin given for 2 weeks prevented and/or minimized loss in RyR2 function induced by untreated diabetes. Compared with

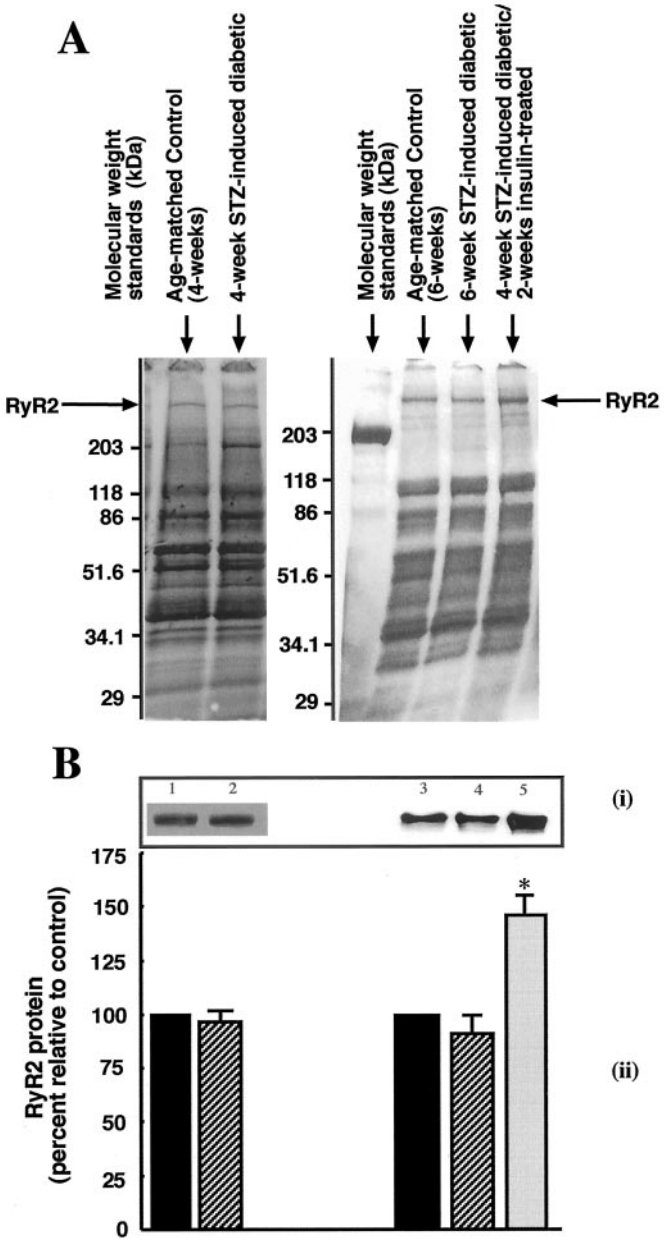


**Fig. 4.** SDS-polyacrylamide gel electrophoresis and Western blots of MV protein from 4- and 6-week STZ-induced, 4-week STZ-induced/2-week insulin-treated diabetic, and age-matched control rat hearts. Briefly, 100 $\mu$g of MV protein from each of control, STZ-induced diabetic, and insulin-treated diabetic rat hearts was dissolved in 30 $\mu$l of gel dissociation medium and electrophoresed for 3.5 h at 150 V using 4 to 20% linear gradient polyacrylamide gels. At the end of this time, gels were either stained with Coomassie dye or transferred onto polyvinylidene difluoride membrane and probed for RyR2 using isoform specific antibodies. A, representative electrophoretogram of MV proteins visualized using Coomassie dye. B, (i) representative auto-radiogram showing intensities of RyR2 from 4-week control and 4-week STZ-induced diabetic rats (lanes 1 and 2) and 6-week age-matched control, 6-week STZ-induced, and 4-week STZ-induced diabetic/2-week insulin-treated diabetic rats (lanes 3, 4, and 5); (ii) intensity of auto-radiogram signals relative to that of age-matched control rats. Values shown are means ± S.E.M. obtained from at least five experiments performed using three different MV preparations for each sample. * denotes value significantly different from control and 6-week STZ-induced diabetic rats.

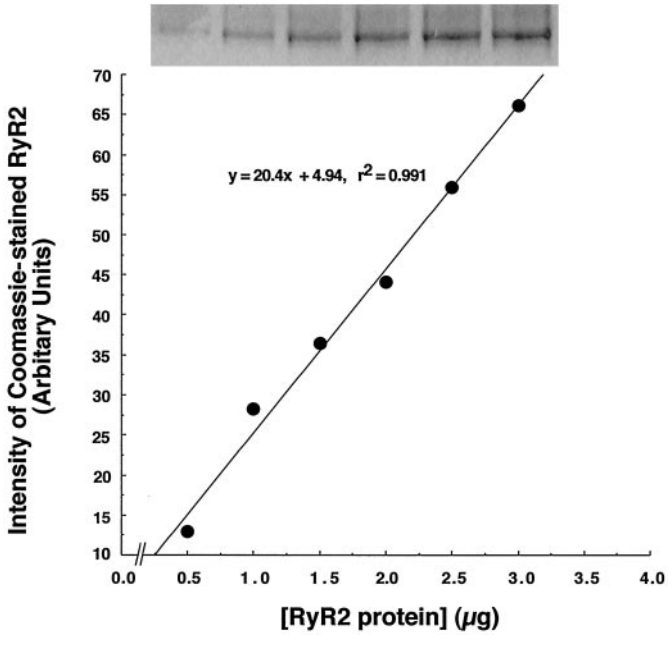


**Fig. 5.** Relationship between intensity of Coomassie staining and RyR2 concentration. Calibration curves were generated to relate the intensity of Coomassie-stained RyR2 in MV preparations to an amount of RyR2 protein. For this, purified RyR2 (0.5 to 3 $\mu$g) were dissolved in gel dissociation medium and electrophoresed on 4 to 20% linear gradient polyacrylamide gels as described. At the end of this time, the gels were Coomassie-stained, destained and then dried. A representative curve generated by plotting intensities of Coomassie-stained RyR2 as a function of RyR2 concentration is shown above.

RyR2 from 6-week STZ-induced diabetic animals, insulin therapy decreases the severity of RyR2 dysfunction induced by diabetes. Thus, insulin treatment slows the progression of RyR2 dysfunction induced by untreated diabetes.

## Discussion

A principal finding of the present study is that 4 and 6 weeks of untreated STZ-induced diabetes produces no apparent alteration in expression of RyR2 in rat hearts. This conclusion is based on studies at the mRNA (reverse transcription-PCR) and protein levels (SDS-polyacrylamide gel electrophoresis and Western blot analyses) of RyR2. Our data also show that at equivalent amounts, RyR2 protein from 6-week STZ-induced diabetic rats bound significantly less [$^3$H]ryanodine (lower $B_{max}$) compared with 6-week age-matched control rats. The decrease in [$^3$H]ryanodine binding is consistent with that reported by Yu et al. (1994) and Imanaga and Uehara (1997), but our data for the first time show that the decrease results from an apparent dysfunction of RyR2 rather than a decrease in the membrane density of the protein. We found no significant loss in activity of RyR2 after 4 weeks of untreated diabetes. It should be pointed out that a decrease in protein activity is not unique to RyR2. Dhalla et al. (1998) reported that diabetes decreases the activity but not expression of SERCA2a in rat hearts.

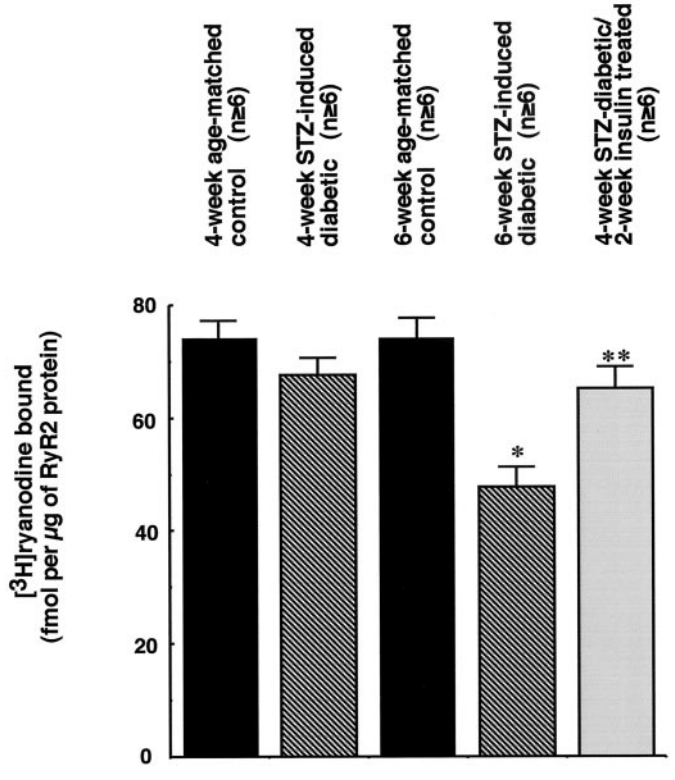


**Fig. 6.** Comparison of functional integrity of RyR2 from 4- and 6-week STZ-induced, 4-week STZ-induced/2-week insulin-treated diabetic, and age-matched control rat hearts. Capacity of RyR2 to bind [$^3$H]ryanodine was used as a measure of its functional integrity. For this, the amount of RyR2 protein in 100 $\mu$g of each MV preparation was determined by interpolating Coomassie-stained intensities on RyR2 calibration curves. RyR2 contents were then normalized to 1 $\mu$g and the adjusted amounts of [$^3$H]ryanodine bound to MV preparation from 4- and 6-week age-matched control rats, 4- and 6-week STZ-diabetic, and 4-week STZ-diabetic/2-week insulin-treated animals were used as measures of their functional integrity. Values shown are means ± S.E.M. for at least six experiments done in duplicate using three different membrane preparations. * denotes significantly different from control rats (4 and 6 weeks), 4-week STZ-diabetic, and insulin-treated. ** denotes significantly different from STZ-diabetic (6 weeks) and age-matched control rats (4 and 6 weeks).

Data from our studies also show that the apparent affinity of ryanodine for RyR2 from control, STZ-induced, and insulin-treated diabetic rat hearts remains essentially unchanged ($IC_{50}$ = 6.9 nM, $K_d$ = 1.04 nM). These data are consistent with those of Yu et al. (1994) but differ from those of Imanaga and Uehara (1997), who found that RyR2 from diabetic dog hearts had a slightly higher affinity for ryanodine compared with age-matched control rats ($K_d$ = 2.4 nM for diabetics compared with 3.8 nM for control animals). Because the latter report listed no standard errors, it is uncertain whether the differences in mean values are statistically significant. It is also possible that differences if real, might be species related.

A decrease in $B_{max}$ is usually suggestive of a decrease in the density of receptor protein available for binding. This may be attributed to a decrease in transcription and/or an increase in degradation rates of the protein. A salient question arising from the present study is how can the same amount of RyR2 protein, displaying the same apparent affinity ($K_d$) bind less [$^3$H]ryanodine (lower $B_{max}$)? Although these results may seem paradoxical at first, they can be rationalized by considering factors that affect the binding of [$^3$H]ryanodine to RyR2. It is generally accepted that binding sites for ryanodine on RyR are located within the transmembrane segments of the channel (Chu et al., 1990; Pessah and Zimanyi 1991; Tinker et al., 1996). It therefore follows that the amount of [$^3$H]ryanodine bound to RyR2 under any given condition is dependent on the amount of time the channels resides in the open state, $P_o$. Several endogenous and exogenous modulators can regulate the latter. For example, we have shown that the binding of [$^3$H]ryanodine to RyR1 (skeletal muscle isoform) is dependent on buffer concentrations of free calcium and $\beta$-$\gamma$-methyleneadenosine 5′-trisphosphate and their effects are biphasic (Emmick et al., 1994). Because our binding affinity assays were performed in the presence of 200 $\mu$M calcium and pH 7.4 one plausible explanation for the decrease in [$^3$H]ryanodine binding could be that the sensitivity of RyR2 to calcium is altered with diabetes. If this is the case then the $P_0$ of RyR2 could be altered and this could lead to a decrease in $B_{max}$ without any change in $K_d$. This effect of diabetes on RyR2 is currently under investigation.

Previous data from our laboratory suggest that there might be two binding sites for ryanodine with affinities in the low nanomolar range on RyR (Bidasee et al., 1995). These two binding sites were uncovered using a radio-iodinated derivative of ryanodine with specific activity of 1400 Ci/mmol, almost 15 times higher than commercially available [$^3$H]ryanodine. If one of these binding sites were to be fully or partially occluded by untreated diabetes, then this could result in a decrease in $B_{max}$. But because the apparent affinities of these two sites are similar (less than 50-fold difference between them), discernible changes in apparent affinity ($K_d$) may not be measurable with low specific activity [$^3$H]ryanodine. It is well known that in diabetes, circulating glucose and intracellular glucose 6-phosphate and fructose 6-phosphate levels increases. These sugars can react nonenzymatically with lysine, hydroxy lysine, and arginine residues on proteins to form Schiff bases (Bunn and Higgins, 1981). Schiff bases rearrange to form Amadori products. Over time

and through a series of random dehydration, oxidation, condensation elimination, and cyclization reactions, Amadori products further rearrange to form advanced glycation end products (AGEs) (Brownlee et al., 1988; Bucala and Cerami, 1992; Bierhaus et al., 1998). Some of these AGEs fluoresce with high quantum yields and are capable of irreversibly cross-linking protein subunits (intra-and intermonomers). Such changes can alter the conformation in such a manner so as to occlude binding site(s) for ryanodine on RyR2.

In preliminary studies, MV from 6-week STZ-diabetic animals were excited with ultraviolet light at 350 nm and emission spectra with $\lambda_{max}$ between 400 and 450 nm (typical of AGEs) were observed (data not shown). These emission spectra were not detected in vesicles prepared from age-matched control animals. Although these data are intriguing, they do not identify the protein on which these compounds are formed or the nature of the AGEs involved. We can conclude, however, that because the electrophoretic mobility of RyR2 from 6-week STZ-diabetic animals is similar to those from control rats and insulin-treated animals, cross-linking AGEs like pentosidine and 4-furanyl-2-furoyl-1*H*-imidazole or analogs thereof may not be formed on RyR2.

Alterations in the oxidative state of sulfhydryl groups on RyR2 can also affect the binding of [$^3$H]ryanodine to RyR2 (Abramson and Salama, 1989). Such changes can be triggered by the increase oxidative stress associated with diabetes (Dhalla et al., 1998). Studies have shown that hydroxy and/or superoxide free radicals are capable of oxidizing critical thiols on the RyR2 and these reactions can lead to changes in conformation of RyR2 (Kawakami and Okabe, 1998) and by extension, alter the binding of [$^3$H]ryanodine to RyR2. More recently, Marengo et al. (1998) showed that the sensitivity of RyR to calcium is dependent on the oxidative state of sulfhydryl groups. However, which of the 89 cysteine residues on each RyR2 monomer might be involved in increasing and/or decreasing $P_0$ remains uncertain.

Our data also show that insulin replacement given after 4 weeks of untreated diabetes increases expression of the RyR2 protein to levels greater than that of age-matched control rats. This increase in the density of RyR2 is consistent with several studies that have shown that insulin replacement increases rates of both protein synthesis and degradation (Abu-Lebdeh and Nair, 1996; Tessari, 2000). Interestingly, after normalization of protein levels we found that RyR2 from insulin-treated animals bound significantly less [$^3$H]ryanodine than that from age-matched control rats. Thus, for a second time the question arises: how can the same amount of RyR2 protein, displaying the same apparent affinity ($K_d$) bind less [$^3$H]ryanodine (lower $B_{max}$)? Although we cannot provide a definite answer to this question, we do know that the functional integrity of RyR2 is compromised in hearts of diabetic rats and that the severity of the dysfunction is dependent on the duration of untreated diabetes. What we also know is that after 14 days on insulin treatment the loss in activity of RyR2 was not completely reversed. Because the common denominator in both instances is time, we believe that a likely explanation for the decrease in $B_{max}$ seen with MV form insulin-treated animals may reside in the half-life of RyR2. If the turnover rate of RyR2 is slow, then RyR2 isolated from insulin-treated rat hearts may consist of a mixture of newly synthesized as well as dysfunctional but not yet degraded RyR2. Thus, although the total amount of RyR2 protein increases, the ability (average) of the protein to bind [$^3$H]ryanodine did not. Assuming that five half-lives are needed for complete protein turnover, then the turnover rate for RyR2 may be in the order of days. This long half-life would allow enough time (days) for Schiff's bases formed on RyR2 to rearrange into Amadori and/or AGEs products. A long half-life may also provide an explanation in support of the deleterious effects of altering the oxidative state of sulfhydryl groups on RyR2.

It is well established that intensity of Coomassie blue R-250 staining differs among proteins (Merril, 1990). Proteins rich in arginine, histidine, and lysine stain more intensely than those containing fewer of these residues because the dye is attracted to these basic groups. It is also well known that glucose, glucose 6-phosphate, fructose 6-phosphate, and other ketose and aldose sugars react nonenzymatically with lysine and arginine residues. In diabetes, the rate at which these nonenzymatic reaction occurs increases (Brownlee et al., 1988). Thus, it is conceivable that if these reactions occur, RyR2 from STZ-diabetic animals may stain less intense with Coomassie blue, than RyR2 from control animals due to fewer free lysine and arginine residues. Fortunately, in this study underestimating RyR2 concentration will result in an underestimation of the degree of RyR2 dysfunction induced by diabetes. Thus, our conclusion that the functional integrity of RyR2 is compromised in diabetes will still hold. We are in the process of purifying RyR2 from control, STZ-diabetic, and insulin treated animals to investigate how much and which of the arginine residues and lysine residues on RyR2 monomer are susceptible to glycation in diabetes.

In conclusion, the present study shows that untreated STZ-diabetes produced a time-dependent decrease in the functional integrity of RyR2 in rat hearts as assessed from their ability to bind [$^3$H]ryanodine. Therefore, in addition to loss of SERCA2a activity, which has already been well documented, loss in activity of RyR2 may also contribute to decrease in cardiac contractility in addition seen in the hearts of STZ-induced diabetic rats.

**Acknowledgments**

We thank Dr. Rod A. Humerickhouse (Department of Medicine, University of Chicago) for purified RyR2. We thank Prof. V. Melih Altan for helpful discussions throughout the study. We also thank James A. Coles, Javid A. Rastegar, and Bruce Henry for technical assistance and Phil Wilson and Lydia Gerbig for valuable help with the illustrations.

**References**

Abu-Lebdeh HS and Nair KS (2000) Protein metabolism in diabetes mellitus. *Bailliere's Clin Endocrinol Metab* **10:**589–601.

Abramson JJ and Salama G (1989) Critical sulfhydryls regulate calcium release from sarcoplasmic reticulum. *J Bioenerg Biomembr* **21:**283–294.

Bell DS (1995) Diabetic cardiomyopathy. A unique entity or a complication of coronary artery disease? *Diabetes Care* **18:**708–714.

Berridge MJ (1997) Elementary and global aspects of calcium signalling. *J Physiol (Lond)* **499:**291–306.

Bers DM (1991) Excitation contraction coupling and cardiac contractile force. Kluwer Academic Press, Boston, MA.

Bidasee KR, Besch HR Jr, Gerzon K, and Humerickhouse RH (1995) Activation and deactivation of the sarcoplasmic reticulum calcium release channel: molecular dissection of mechanisms via novel semi-synthetic ryanoids. *Mol Cell Biochem* **149/150:**145–159.

Bidasee KR, Maxwell A, Reynolds WF, Patel V, and Besch HR Jr (2000) Tectoridins modulate skeletal and cardiac muscle sarcoplasmic reticulum calcium-release channels. *J Pharmacol Exp Ther* **293:**1074–1083.

Bierhaus A, Hofmann MA, Ziegler R, and Nawroth PP (1998) AGEs and their

interaction with AGE-receptors in vascular disease and diabetes mellitus. I. The AGE concept. *Cardiovasc Res* **37:**586–600.
Brownlee M, Cerami A, and Vlassara H (1988) Advanced glycosylation end products in tissues and the biochemical basis of diabetic complications. *N Engl J Med* **319:**315–321.
Brownsey RW, Boone AN, and Allard MF (1997) Actions of insulin on the mammalian heart: metabolism, pathology and biochemical mechanisms. *Cardiovasc Res* **34:**3–24.
Bucala R and Cerami A (1992) Advanced glycosylation: chemistry, biology and implications for diabetes and aging. *Adv Pharmacol* **23:**1–34.
Bunn HF and Higgins PJ (1981) Reactions of monosaccharides with proteins: possible evolutionary significance. *Science (Wash DC)* **213:**222–224.
Cheng Y-C and Prusoff WH (1973) Relationship between the inhibition constant (K1) and the concentration of inhibitor which causes 50 percent inhibition (I50) of an enzymatic reaction. *Biochem Pharmacol* **22:**3099–3108.
Chu A, Diaz-Munoz M, Hawkes MJ, Brush K, and Hamilton SL (1990) Ryanodine as a probe for the functional state of the skeletal muscle sarcoplasmic reticulum calcium release channel. *Mol Pharmacol* **37:**735–741.
Davidoff AJ and Ren J (1997) Low insulin and high glucose induce abnormal relaxation in cultured adult rat ventricular myocytes. *Am J Physiol* **272:**H159–H167.
de la Bastie D, Levitsky DL, Rappaport L, Mercadier JJ, Marotte F, Wisnewsky C, Brovkovich V, Schwartz K, and Lompre AM (1990) Function of the sarcoplasmic reticulum and expression of its $Ca^{2+}$-ATPase gene in pressure overload-induced cardiac hypertrophy in the rat. *Circ Res* **66:**554–564.
Dhalla NS, Lui X, Panagia V, and Takeda N (1998) Subcellular remodeling and heart dysfunction in chronic diabetes. *J Cardiovasc Res* **40:**239–247.
Dinçer UD, Bidasee KR, Güner S, Tay A, Ozcelikay AT, and Altan VM (2001) The effects of diabetes on expression of $\beta_1$-, $\beta_2$- and $\beta_3$- adrenoceptors in rat hearts. *Diabetes* **50:**455–461.
Emmick JT, Kwon S, Bidasee KR, Besch KT, and Besch HR Jr (1994) Dual effects of Suramin on calcium fluxes across sarcoplasmic reticulum membrane vesicles. *J Pharmacol Exp Ther* **269:**717–724.
Ganguly PK, Pierce GN, Dhalla KS, and Dhalla NS (1983) Defective sarcoplasmic reticular calcium transport in diabetic cardiomyopathy. *Am J Physiol* **244:**E528–E535.
Imanaga I and Uehara A (1997) Dysfunction of cardiac sarcoplasmic reticulum in diabetic animal (Abstract). *J Mol Cell Cardiol* **29:**A300.
Kawakami M and Okabe E (1998) Superoxide anion radical-triggered $Ca^{2+}$ release from cardiac sarcoplasmic reticulum through ryanodine receptor $Ca^{2+}$ channel. *Mol Pharmacol* **53:**497–503.
Kiriazis H and Kranias EG (2000) Genetically engineered models with alterations in cardiac membrane calcium-handling proteins. *Annu Rev Physiol* **62:**321–351.
Klautz RJ, Baan J, and Teitel DF (1997) The effect of sarcoplasmic reticulum blockade on the force/frequency relationship and systolic contraction patterns in the newborn pig heart. *Pfleug Arch Eur J Physiol* **435:**130–136.
Lopaschuk GD, Katz S, and McNeill JH (1983) The effect of alloxan- and streptozotocin-induced diabetes on calcium transport in rat cardiac sarcoplasmic. The possible involvement of long chain acylcarnitines. *Can J Physiol Pharmacol* **61:**439–448.
Mahgoub MA and Abd-Elfattah AS (1998) Diabetes mellitus and cardiac function. *Mol Cell Biochem* **180:**59–64.
Marengo JJ, Hildago C, and Bull R (1998) Sulfhydryl oxidation modifies the calcium dependence of ryanodine-sensitive calcium release channel of excitable cells. *Biophys J* **74:**1236–1277.
Merril CR (1990) Gel staining technique, in *Guide to Protein Purification* (Duetscher MP ed) pp. 477–488, Academic Press, San Diego, CA.
Otsu K, Willard HF, Khanna VK, Zorato F, Green NM, and MacLennan DH (1990) Molecular cloning of cDNA encoding the $Ca^{2+}$release channel (ryanodine receptor) of rabbit cardiac muscle sarcoplasmic reticulum. *J Biol Chem* **265:**13472–13483.
Pessah IN and Zimanyi I (1991) Characterization of multiple [$^3$H]ryanodine binding sites on the $Ca^{2+}$ release channel of sarcoplasmic reticulum from skeletal and cardiac muscle: evidence for a sequential mechanism in ryanodine action. *Mol Pharmacol* **39:**679–689.
Rubler S, Dlugash J, Yuceoglu YZ, Kumral T, Branwood AW, and Grishman A (1972) New type of cardiomyopathy associated with diabetic glomerulo-sclerosis. *Am J Cardiol* **30:**595–602.
Russ M, Reinauer H, and Eckel J (1991) Diabetes-induced decrease in the mRNA coding for sarcoplasmic reticulum $Ca^{2+}$-ATPase in adult rat cardiomyocytes. *Biochem Biophys Res Commun* **178:**906–912.
Teshima Y, Takahashi N, Saikawa T, Hara M, Yasunaga S, Hidaka S, and Sakata T (2000) Diminished expression of sarcoplasmic reticulum Ca$^{(2+)}$-ATPase and ryanodine sensitive Ca$^{(2+)}$ channel mRNA in streptozotocin-induced diabetic rat heart. *J Mol Cell Cardiol* **32:**655–664.
Tessari P (2000) Changes in protein, carbohydrate, and fat metabolism with aging: possible role of insulin. *Nutr Rev* **58:**11–19.
Tinker A, Sutko JL, Ruest L, Deslongchamp P, Welch W, Airey JA, Gerzon K, Bidasee KR, Besch HR Jr, and Williams AJ (1996) The effects of ryanodine derivatives on the channel properties of the ryanodine receptor. *Biophys J* **70:**2110–2119.
Tunwell RE, Wickenden C, Bertrand BM, Shevchenko VI, Walsh MB, Allen PD, and Lai FA (1996) The human cardiac muscle ryanodine receptor-calcium release channel: identification, primary structure and topological analysis. *Biochem J* **318:**477–487.
Wolfe RR (2000) Effects of insulin on muscle tissue. *Curr Opin Clin Nutr Metab Care* **3:**67–71.
Yu Z and McNeill JH (1991) Force-interval relationship and its response to ryanodine in streptozotocin-induced diabetic rats. *Can J Physiol Pharmacol* **69:**1268–1276.
Yu Z, Tibbits GF, and McNeill JH (1994) Cellular functions of diabetic cardiomyocytes: contractility, rapid-cooling contracture, and ryanodine binding. *Am J Physiol* **266:**H2082–H2089.
Zarain-Herzberg A, Yano K, Elimban V, and Dhalla NS (1994) Cardiac sarcoplasmic reticulum $Ca^{2+}$-ATPase expression in streptozotocin-induced diabetic rat heart. *Biochem Biophys Res Commun* **203:**113–120.

**Address correspondence to:** Dr. Keshore R. Bidasee, Department of Pharmacology and Toxicology, 635 Barnhill Drive MS A417, Indianapolis, IN 46202-5120. E-mail: kbidase@iupui.edu